AlGaN metal-semiconductor-metal ultraviolet photodetectors on sapphire substrate with a low-temperature AlN buffer layer

Junqin Zhang (张军琴)*, Yintang Yang (杨银堂), and Hujun Jia (贾护军)

Ministry of Education, Key Laboratory of Wide Band Gap Semiconductor Materials and Devices, Xidian University, Xi'an 710071, China

**Corresponding author: zhangjq@mail.xidian.edu.cn*

Received April 8, 2013; accepted September 4, 2013; posted online September 29, 2013

Unintentionally doped AlGaN thin films are grown on c-plane (0001) sapphire substrate by metal-organic chemical vapor deposition, and low-temperature AlN is deposited onto sapphire substrate used as a buffer layer. AlGaN metal-semiconductor-metal ultraviolet photodetectors with Ni/Au interdigitated contact electrodes are then fabricated by lift-off technology. The dark current of the AlGaN photodetectors is 5.61×10^{-9} A at 2-V applied bias and the peak response occurrs at 294 nm.

OCIS codes: 230.5160, 230.0040.

doi: 10.3788/COL201311.102304.

Ultraviolet (UV) photodetectors have the advantages of concealment, low false alarm rate, and anti-electromagnetic interference[1]. Thus, these devices are widely applied in the field of radar technology, communications, aerospace, automotive, and so on. Meanwhile, the semiconductor material GaN has the advantages of wide direct bandgap, high breakdown field, high saturation velocity, and high heat conductivity. Hence, GaN is a very attractive material for applications in high-temperature, high-power, high-frequency optoelectronics, and anti-radiation devices[2−4]. In particular, the energy gap of $Al_xGa_{1-x}N$ can be tuned from 3.4 ($x = 0$) to 6.2 eV ($x = 1$) by altering the Al composition, thereby enabling the selection of the cutoff wavelength from 365 to 200 nm[5−7]. Accordingly, AlGaN has become one of the most promising materials for the fabrication of UV photodetectors[8,9]. In the field of UV detection, AlGaN materials grown on sapphire substrates are of particular interest because of the high performance of GaN-based UV photodetectors.

Different AlGaN UV detectors have been proposed, such as Schottky barrier detectors[10,11], metal-semicon ductor-metal (MSM) detectors[12,13], p-n and p-i-n detectors[14−16], as well as heterojunction detectors[17,18]. Among them, MSM photodetectors are an attractive choice for UV detectors because they are easily fabricated, high speed, and suitable for integration in optoelectronic integrated circuits[19,20]. In back-to-back Schottky MSM photoconductors, large area solar-blind $Al_{0.4}Ga_{0.6}N$ photodetectors with ultra-low dark current have been reported, the dark current is less than 0.2 pA at 20 V bias[21]. In this letter, AlGaN layers were grown on sapphire substrates with a low-temperature AlN buffer layer, and then AlGaN MSM photodetectors were fabricated using Ni/Au.

The AlGaN samples used in this study were prepared by metal-organic chemical vapor deposition (MOCVD) on 2-inch c-plane (0001) sapphire substrates. Trimethyl aluminum (TMAl), trimethyl gallium (TMG), and ammonia (NH_3) were used as the source materials of Al, Ga, and N, respectively. High-purity hydrogen (H_2) was used as the carrier gas. The sapphire substrates were cleaned prior to the epilayer growth, and then a 30-nm low-temperature AlN buffer layer was deposited onto this sapphire substrate at 750 °C. Afterwards, the temperature was increased to 1100 °C to grow 820-nm unintentionally doped AlGaN epitaxial layers. The reactor pressure was set to 75 mbar during the processing of the AlN buffer layer and the growth of the AlGaN epitaxial layers. The Al content of $Al_xGa_{1-x}N$ was designed to be about 30%. The typical room temperature carrier concentration of the unintentionally doped AlGaN epitaxial layers was 10^{16} cm^{-3}. The film thickness was monitored using the reflection detection curve obtained during growth.

The MSM AlGaN photodetectors consisted of two interdigitated contact electrodes fabricated by standard lithography and lift-off technique. Firstly, photoresist was coated on the AlGaN epitaxial layer, and then the contact pattern of interdigitated contact electrodes were defined by standard lithography. Then, Ni/Au (20 nm/80 nm) contact layers were deposited onto the samples to serve as a Schottky contact and the interdigitated contact electrodes were formed by lift-off technology. To improve the stability of the Schottky contacts, the samples were subsequently annealed in N_2 atmosphere at 550 °C for 60 s. Subsequently, a 170-nm SiO_2 layer was deposited onto the surface of the AlGaN layer and the metal fingers. Here, the SiO_2 layer was used as an antireflection layer as well as for protecting the metal fingers. Subsequently, the via was formed by lithography and etch. Finally, Ti/Au (10 nm/50 nm) was deposited to serve as an electroplating pathway, and Au (2000 nm) was subjected to selective plating to serve as bonding pads. To enhance surface bonding between the Au and SiO_2 layers, Ti was used as a transition layer in the bonding pads. The fabrication of AlGaN MSM photodetectors was completed after the process of substrate thinning, scribing, bonding, and packaging.

The schematic of the AlGaN MSM photodetector is

 © 2013 Chinese Optics Letters

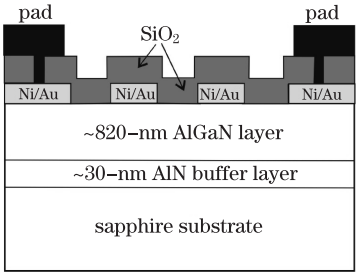

Fig. 1. Schematic of AlGaN MSM photodetectors.

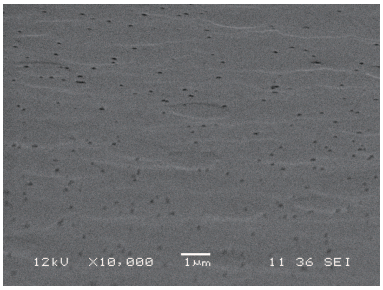

Fig. 2. SEM of AlGaN epitaxial layers.

shown in Fig. 1. The Ni/Au fingers of the interdigitated contact electrodes were 3-μm wide and 465-μm long, with a spacing of 6 μm. The bonding pad area of the fabricated photodetectors was 160 ×160 (μm).

The surface morphology of AlGaN epitaxial layers was characterized by scanning electron microscopy (SEM). The crystalline structure and crystal quality of AlGaN film were characterized by X-ray diffraction (XRD) and Raman spectroscopy. A Keithley-2400 semiconductor parameter analyzer was used to measure the dark current-voltage ($I-V$) characteristics of these photodetectors at room temperature. For spectral response measurements, a Xe arc lamp was used as the light source, and the detector was illuminated from the front side.

Figure 2 shows the surface morphology of the AlGaN epitaxial layers. Numerous dark spots are observed on the AlGaN surface, which can be attributed to the threading dislocation in the epitaxial layers[22]. Some pit defects on AlGaN surface are also observed, which may be due to the irregular surface defects on the substrates introduced during polishing and incompletely removed by chemical cleaning.

The structural properties of the AlGaN epitaxial layers were investigated by XRD measurements using an X'Pert Pro MPD X-ray diffractometer from PANalytical and Cu target as a radiation source. Figure 3 shows the XRD spectrum of the AlGaN film measured at room temperature.

A prominent diffraction peak located at $2\theta = 35°$, which corresponded to AlGaN (0002), was observed[23]. The strong intensity of the XRD peak indicated that highly (0002) oriented AlGaN thin films were obtained using the low-temperature AlN buffer layer on sapphire substrates. The full-width at half-maximum (FWHM) of the AlGaN (0002) peaks was around 0.09°. This value is not a satisfied one for the AlGaN epilayer with a good crystal quality and the surface morphology of it proved this issue. Two other peaks were observed in Fig. 3. The AlN buffer layer-related peak appeared at $2\theta = 36.1°$, whereas the peak located at $2\theta = 41.7°$ corresponded to sapphire substrate.

Figure 4 shows the Raman spectrum of the AlGaN epitaxial layers measured at room temperature using an InVia laser Raman spectrometer under the $Z(X,X)\overline{Z}$ configuration. The peak at 578.4 cm^{-1} was dominant in the spectrum, which corresponded to the E_2 mode of the AlGaN epitaxial layer. The mode near 807 cm^{-1} was the A_1(LO) mode of AlGaN. Two other clear features were observed at 658.7 and 749.8 cm^{-1}, respectively. Among them, the peak at 658.7 cm^{-1} was the E_2 phonon mode of AlN, whereas the peak at 749.8 cm^{-1} came from sapphire substrate.

Figure 5 shows microphotographs of the completed MSM photodetectors. The MSM Schottky photodetectors consisted of two interdigitated contact electrodes that were clear and not interconnected with one another.

Figure 6 shows the room temperature $I-V$ characteristics of the fabricated MSM AlGaN photodetectors measured without illumination. With a 2-V applied bias, the dark currents of the photodetectors was 5.61×10^{-9}

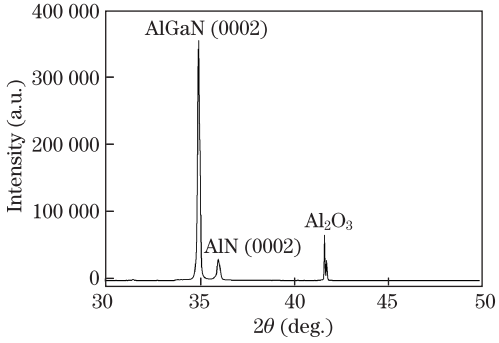

Fig. 3. XRD pattern of the AlGaN epitaxial layers grown on sapphire substrate.

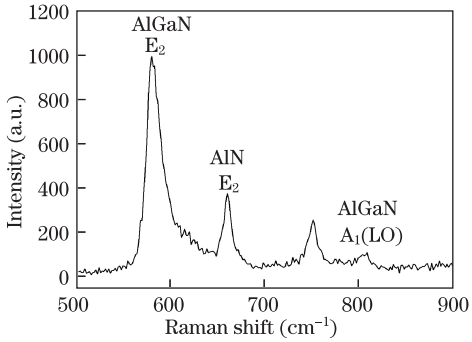

Fig. 4. Raman spectrum of AlGaN epitaxial layers.

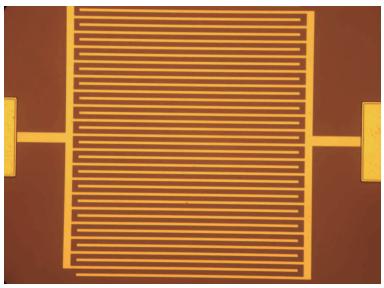

Fig. 5. SEM image of the fabricated AlGaN MSM photodetectors.

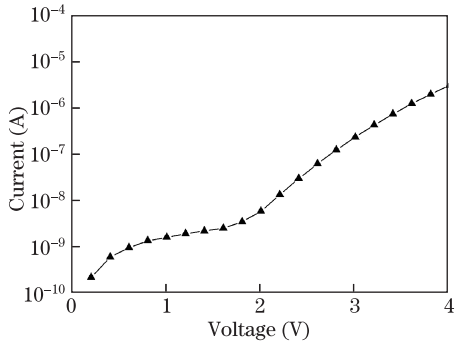

Fig. 6. $I-V$ characteristics of the fabricated AlGaN photodetectors without illumination.

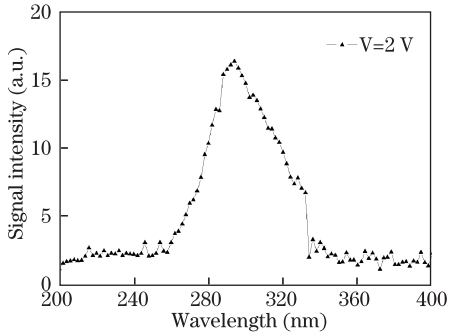

Fig. 7. Spectral response of the fabricated AlGaN MSM photodetectors (without calibration).

A, which was higher than that reported in Ref. [24]. This high dark current is attributed to the unsatisfied crystal quality, the defect and impurities in the unintentionally doped AlGaN layers[25]. Some other factors, such as surface passivation and electrode contact potential may also incurred higher dark currents.

Figure 7 shows the spectral response of the fabricated AlGaN MSM photodetectors with 2-V applied bias measured at room temperature. No calibration standard detector was used in the test system; hence, the relative spectral response of the AlGaN photodetectors was measured. As shown in Fig. 7, the spectral response curve exhibited a sharp cutoff at the absorption edge and the peak response occurred at 294 nm. But it was found that the cutoff was not so sharp like some references[26], which might be related to absorption in defects or partial regions with different compositions in the ternary alloy[27].

In conclusion, AlGaN films are grown on 2-inch sapphire substrate by MOCVD, and AlGaN MSM UV photodetectors with Ni/Au contacts are fabricated using standard lithography and lift-off technology. The AlGaN film properties are investigated by XRD and Raman scattering spectroscopy analyses. $I-V$ and spectral response characteristics of the AlGaN MSM photodetectors are also determined. At 2-V applied bias, the dark currents of AlGaN photodetectors is 5.61×10^{-9} A and the peak response appeared at 294 nm.

This work was supported by the National Natural Science Foundation of China (No. 61006052) and the Fundamental Research Funds for the Central Universities (No. K5051325009).

References

1. X. Du, B. Chang, Y. Qian, and P. Gao, Chin. Opt. Lett. **9,** 010401 (2011).
2. T. Nomura, H. Kambayashi, M. Masuda, S. Ishii, N. Ikeda, J. Lee, and S. Yoshida, IEEE Tran. Electron Dev. **53,** 2908 (2006).
3. W. Saito, Y. Takada, M. Kuraguchi, K. Tsuda, and I. Omura, IEEE Tran. Electron Dev. **53,** 356 (2006).
4. J. M. wang, K. F. Lee, and H. L. wang, J. Phys. Chem. Solids **69,** 752 (2008).
5. M. S. Shur, R. Gaska, and A. Bykhovski, Solid State Electron. **43,** 1451 (1999).
6. D. Walker, A. Saxler, P. Kung, X. Zhang, M. Hamilton, J. Diaz, and M. Razeghi, Appl. Phys. Lett. **72,** 3303 (1998).
7. J. Q. Zhang, Y. T. Yang, C. C. Chai, Y. J. Li, and H. J. Jia, J. Semicond. **29,** 2187 (2008).
8. C. H. Chen, S. J. Chang, Y. K. Su, G. C. Chi, J. Y. Chi, C. A. Chang, J. K. Sheu, and J. F. Chen, IEEE Photon. Technol. Lett. **13,** 848 (2001).
9. I. Ferguson, C. A. Tran, R. F. Karlicek Jr, Z. C. Feng, R. Stall, S. Liang, Y. Lu, and C. Joseph, Mater. Sci. Eng. B-adv. **50,** 311 (1997).
10. J. Li, M. Zhao, X. F. Wang, Phys. B **405,** 996 (2010).
11. T. K. Ko, S. J. Chang, Y. K. Su, M. L. Lee, and C. S. Chang, J. Cryst. Growth **283,** 68 (2005).
12. P. C. Chang, C. H. Chen, S. J. Chang, Y. K. Su, C. L. Yu, P. C. Chen, and C. H. Wang, Photon. Nanostruct. **5,** 53 (2007).
13. M. Cökkayas, S. Butun, T. Tut, N. Biyikli, and E. Ozbay, Photon. Nanostruct. **5,** 53 (2007).
14. S. S. Liu, P. W. Li, W. H. Lan, and Y. C. Cheng, Mater. Sci. Eng. B-adv. **126,** 33 (2006).
15. N. Biyikli, I. Kimukin, O. Aytur, and E. Ozbay, IEEE Photon. Technol. Lett. **16,** 1718 (2004).
16. A. Asgari, E. Ahmadi, and M. Kalafi, Microelectron. J. **40,** 104 (2009).
17. G. Parish, M. Hansen, B. Moran, S. Keller, S. P. DenBaars, and U. K. Mishra, Phys. Stat. Sol. A **188,** 297 (2001).
18. S. V. Averine, P. I. Kuznetzov, V. A. Zhitov, and N. V. Alkeev, Solid State Electron. **52,** 618 (2008).
19. S. Wang, T. Li, J. M. Reifsnider, B. Yang, C. Collins, A. L. Holmes, and J. C. Campbell, IEEE J. Quantum Electron. **36,** 1262 (2000).
20. C. K. Wang, S. J. Chang, Y. K. Su, Y. Z. Chiou, C. S. Chang, T. K. Lin, H. L. Liu, and J. J. Tang, Semicond. Sci. Technol. **20,** 485 (2005).
21. F. Xie, H. Lu, D. J. Chen, P. Han, R. Zhang, Y. D. Zheng, L. Li, W. H. Jiang, and C. Chen, Electron. Lett. **47,** 930 (2011).
22. R. W. Chuang, C. L. Yu, S. J. Chang, P. C. Chang, J. C. Lin, and T. M. Kuan, J. Cryst. Growth **308,** 252 (2007).
23. X. L. Wang, C. M. Wang, G. X. Hu, H. L. Xiao, C. B. Fang, J. X. Wang, J. X. Ran, J. P. Li, J. M. Li, and Z. G. Wang, J. Cryst. Growth **298**, 791 (2007).
24. M. Mosca, J. Reverchon, N. Grandjean, and J. Duboz, IEEE J. Sel. Top. Quantum **10,** 752 (2004).
25. S. J. Chang, T. K. Ko, J. K. Sheu, S. C. Shei, W. C. Lai, Y. Z. Chiou, Y. C. Lin, C. S. Chang, W. S. Chen, and C. F. Shen, Sensor. Actuat. A-phys. **135,** 502 (2007).
26. E. Munoz, E. Monroy, J. L. Pau, F. Calle, E. Calleja, F. Omnes, and P. Gibart, Phys. Stat. Solid. A **180,** 293 (2000).
27. Y. Z. Chiou, Y. C. Lin, and C. K. Wang, IEEE Electron. Dev. Lett. **28,** 264 (2007).